Int J Cardiovasc Imaging (2016) 32:461–467
DOI 10.1007/s10554-015-0792-x

ORIGINAL PAPER

Blood flow characteristics in the ascending aorta after TAVI compared to surgical aortic valve replacement

Ralf Felix Trauzeddel[1,2] · Ulrike Löbe[3] · Alex J. Barker[4,5] · Carmen Gelsinger[3] · Christian Butter[3] · Michael Markl[4,5] · Jeanette Schulz-Menger[1,2] · Florian von Knobelsdorff-Brenkenhoff[1,2]

Received: 5 August 2015 / Accepted: 15 October 2015 / Published online: 22 October 2015

Abstract Ascending aortic blood flow characteristics are altered after aortic valve surgery, but the effect of transcatheter aortic valve implantation (TAVI) is unknown. Abnormal flow may be associated with aortic and cardiac remodeling. We analyzed blood flow characteristics in the ascending aorta after TAVI in comparison to conventional stented aortic bioprostheses (AVR) and healthy subjects using time-resolved three-dimensional flow-sensitive cardiovascular magnetic resonance imaging (4D-flow MRI). Seventeen patients with TAVI (Edwards Sapien XT), 12 with AVR and 9 healthy controls underwent 4D-flow MRI of the ascending aorta. Target parameters were: severity of vortical and helical flow pattern (semiquantitative grading from 0 = none to 3 = severe) and the local distribution of systolic wall shear stress ($WSS_{systole}$). AVR revealed significantly more extensive vortical and helical flow pattern than TAVI ($p = 0.042$ and $p = 0.002$) and controls ($p < 0.001$ and $p = 0.001$). TAVI showed significantly more extensive vortical flow than controls ($p < 0.001$). Both TAVI and AVR revealed marked blood flow eccentricity (64.7 and 66.7 %, respectively), whereas controls showed central blood flow (88.9 %). TAVI and AVR exhibited an asymmetric distribution of $WSS_{systole}$ in the mid-ascending aorta with local maxima at the right anterior aortic wall and local minima at the left posterior wall. In contrast, controls showed a symmetric distribution of $WSS_{systole}$ along the aortic circumference. Blood flow was significantly altered in the ascending aorta after TAVI and AVR. Changes were similar regarding $WSS_{systole}$ distribution, while TAVI resulted in less helical and vortical blood flow.

Keywords Magnetic resonance imaging · Aorta · Aortic valve replacement · Shear stress · Transcatheter aortic valve implantation · 4D-flow

✉ Florian von Knobelsdorff-Brenkenhoff
florian.von-knobelsdorff@charite.de

[1] Working Group Cardiovascular Magnetic Resonance, Experimental and Clinical Research Center, A Joint Cooperation Between the Charité Medical Faculty and the Max-Delbrueck Center for Molecular Medicine, Charité Medical University Berlin, Lindenberger Weg 80, 13125 Berlin, Germany

[2] Department of Cardiology and Nephrology, HELIOS Klinikum Berlin Buch, Berlin, Germany

[3] Department of Cardiology, Immanuel Klinikum Bernau, Heart Center Brandenburg, Bernau, Germany

[4] Department of Radiology, Feinberg School of Medicine, Northwestern University, Chicago, IL, USA

[5] Department of Biomedical Engineering, McCormick School of Engineering, Northwestern University, Chicago, IL, USA

Introduction

Transcatheter aortic valve implantation (TAVI) has become an accepted method for treating patients with severe aortic stenosis who are not eligible or at high risk for conventional surgical aortic valve replacement (AVR) [1–3]. Previous studies have demonstrated that changes in the geometry of the aortic valve such as bicuspid valves or AVR result in altered blood flow patterns and parameters [4, 5]. These abnormalities may be associated with aortic remodeling and increased cardiac afterload [6, 7]. As there is little knowledge about the effect of TAVI on the global patterns of blood flow in the ascending aorta, the aim of this study was to analyze the blood flow characteristics in the ascending aorta after TAVI in comparison to AVR with a stented aortic bioprosthesis and healthy controls using

time-resolved, three-dimensional, flow-sensitive magnetic resonance (4D-flow MRI). This technique allows for the visualization of vortical and helical blood flow patterns as well as quantifying local flow velocities and WSS [8]. We hypothesize that both AVR and TAVI will result in altered hemodynamics compared to controls.

Materials and methods

Study sample

The local ethics committee approved the study. Inclusion criteria to enter the study were either carrier of any stented aortic bioprosthesis or an Edwards Sapien XT TAVI valve, or a healthy status with no signs or history of a heart disease. Exclusion criteria were common contraindications for MRI, atrial fibrillation, and concomitant aortic surgery. Written informed consent was obtained from all individuals. Twenty-three consecutive patients with TAVI with an Edwards Sapien XT® prosthesis were prospectively enrolled. This study focused on the Edwards Sapien XT® as at the time of study enrollment this was the preferred device in the cooperating TAVI center. Six patients were excluded from further analysis due to extensive respiratory motion and thus inefficient respiratory navigator. The data of 12 patients with stented bioprosthesis and 9 healthy controls were retrospectively analyzed from a previous study [5]. Two cases with stented bioprosthesis of the previous study were not included due to technical incompatibility of the data with the present analysis software. All TAVI patients had severe symptomatic aortic stenosis as the main diagnosis leading to the intervention. In AVR, 2 had severe aortic regurgitation and 10 had severe aortic stenosis. The characteristics of the study participants are summarized in Table 1.

Image acquisition protocol

Images were acquired in a high-volume clinical and research CMR center (3000 exams/year) by specialized technicians as previously described [5]. All subjects underwent a CMR examination at a 1.5 Tesla MR scanner (Magnetom Avanto, Siemens Healthcare, Erlangen, Germany). A 12-channel anterior body array coil was used for signal reception and the body coil for signal transmission. 4D-flow was acquired using a sagittal oblique volume covering the thoracic aorta. Prospective ECG gating was used with a respirator navigator placed on the lung-liver interface. The following scan parameters were chosen for the healthy controls and the AVR group: echo time [TE] = 2.3 ms, repetition time [TR] = 4.8 ms, bandwith = 440 Hz/pixel, acceleration mode GRAPPA with factor 2 to 5, reference lines = 24, flip angle $\alpha = 9°$, temporal resolution = 38.4 ms, voxel size = 2.1 × 2.4 × 2.2 mm^3, velocity encoding = 1.5–2.5 m/s. For the TAVI sample, an improved technique to accelerate image acquisition was used. Previous studies have demonstrated that the results of both techniques are interchangeable [9]. [TE] = 2.6 ms, [TR] = 4.8 ms, bandwith = 401 Hz/pixel, acceleration mode GRAPPA with factor 5, reference lines = 24, flip angle $\alpha = 9°$, temporal resolution = 42.0 ms, voxel size = 1.8 × 1.8 × 2.6 mm^3, velocity encoding = 1.5–2.5 m/s.

Conventional ECG-gated, breath-held steady-state free-precession (SSFP) cine imaging was performed to quantify left ventricular function and the geometric orifice area (GOA) of the aortic valve and bioprostheses, respectively [10]. The GOA of TAVI could not be determined from SSFP images due to significant artefacts, but was taken from the literature [11, 12]. Axial SSFP still images of the thorax were used to estimate the size of the ascending aorta at the level of the pulmonary bifurcation [13].

Processing and analysis of the images

All 4D-flow MRI data were processed by an experienced 4D flow reader (M.D., 5 years experiences with 4D flow) as previously described [8], and supervised by an experienced SCMR level III reader and instructor. Briefly, data were corrected for noise, eddy currents and velocity aliasing (MatLab; The MathWorks, Natick, MA, USA) [14]. In a second step, a 3D phase contrast MR angiogram was calculated based on the flow measurements to position the analysis planes and to visualize the blood flow (EnSight, CEI, Apex, NC). Three planes were positioned perpendicular to the longitudinal axis of the aortic wall: at the level of the sinotubular junction (S1), in the ascending aorta at the level of the pulmonary bifurcation (S2), and proximal to the brachiocephalic trunk (S3). The position of S1 was selected such that it was high enough to avoid signal artifact caused by the presence of the metal in the prosthetic stents. These analysis planes were exported into previously reported software for the segmentation and calculation of the blood flow parameters (MatLab; The MathWorks, Natick, MA, USA) [14].

Left ventricular function quantification and planimetry of the GOA were achieved by manual segmentation using commercial software (CVI[42], Circle Cardiovascular Imaging, Calgary, Canada). Assessment of the aortic diameter was done at the in ascending aorta at the level of the pulmonary bifurcation [13].

Table 1 Baseline characteristics of the study participants

Parameter	TAVI	AVR	Controls	*p* value
n	17	12	9	
Sex (females/males)	8/9	4/8	1/8	
Age (years)	77 ± 7	76 ± 4	55 ± 16	0.001
Native valvular lesion	Stenosis (n = 10), mixed (n = 7)	Stenosis (n = 6), regurgitation (n = 2), mixed (n = 4)	–	
Prosthetic types	Sapien XT (n = 17),	Hancock (n = 4), Labcore (n = 1); Perimount (n = 2) Mitroflow (n = 2), unknown (n = 3)	–	
Labeled valve size	25.8 ± 2.2	23.2 ± 2.2	–	0.012
Geometric orifice area (cm^2)	1.9 ± 0.3	1.5 ± 0.5	4.0 ± 0.8	< 0.001
Geometric orifice area index (cm^2/m^2)	0.9 ± 0.3	0.8 ± 0.2	2.0 ± 0.3	< 0.001
LV enddiastolic volume (ml)	157.0 ± 63.2	149.9 ± 61.8	139.6 ± 41.4	0.870
LV mass (g)	175.7 ± 59.3	165.2 ± 55.1	129.2 ± 25.3	0.079
LV stroke volume (ml)	87.9 ± 33.1	84.9 ± 32.3	91.4 ± 28.2	0.796
LV ejection fraction (%)	57.2 ± 10.1	58.0 ± 10.9	65.9 ± 6.1	0.038
Ascending aortic diameter (mm)	34.8 ± 3.1	38.5 ± 4.4	30.7 ± 4.8	0.002

Results are given as mean ± standard deviation or as frequencies. The *p* values are tested by the Kruskal–Wallis analysis

LV left ventricular

Helical and vortical blood flow pattern in the ascending aorta

Blood flow patterns were semi-quantitatively evaluated using pathline movies and classified as vortical and helical as previously described [5]. In short, helical and vortical flow were graded in 4 categories: 0 = none, 1 = mild, 2 = moderate, 3 = severe at the mid-ascending aorta [5].

Blood flow eccentricity in the ascending aorta

Blood flow was semi-quantitatively graded as central or mild eccentric or marked eccentric as previously described [5, 15]. A central flow was characterized if the flow occupied the majority of the vessel lumen. A mild eccentric flow occupied two-thirds to one-third of the vessel and a marked eccentric flow occupied one-third or less of the vessel.

Wall shear stress in the ascending aorta

WSS was computed as previously described [14] by using a B-spline interpolation model to obtain the velocity derivatives necessary to compute the deformation tensor at the wall. WSS was subsequently found via the relation $\vec{\tau} = 2\mu\dot{\vec{\varepsilon}} \cdot \vec{n}$, where $\vec{\tau}$ is WSS, μ is the dynamic viscosity (assumed constant at 4.5 cP), $\dot{\varepsilon}$ is the deformation tensor, and $\vec{n}$ is the normal unit vector to the vessel wall. Quantification of systolic WSS ($WSS_{systole}$; unit N/m^2) was performed for 8 regional segments along the aortic circumference for each analysis plane S1–S3. Regional WSS was averaged over three time points.

Statistical analysis

Analysis of the data was performed using SPSS 22 (IBM, Armonk, US). Graphics were created using PRISM 5 (GraphPad Software Inc, San Diego, California, US) and plug-in software for MatLab. Categorical data are expressed as percentages, continuous data as mean ± standard deviation (SD). The three groups (TAVI, AVR, controls) were compared using the Kruskal–Wallis test. Post-hoc analysis included the Mann–Whitney-*U* test. Statistical significance was set at a probability level of <0.05.

Results

Baseline characteristics

Table 1 summarizes the baseline characteristics of the study participants. Healthy controls were significantly younger than patients with AVR ($p = 0.002$) and TAVI ($p = 0.001$) and had significantly larger GOA ($p < 0.001$) and GOA index ($p < 0.001$). They also had a smaller aortic diameter than AVR ($p = 0.003$) and TAVI ($p = 0.021$). AVR and TAVI were not different regarding age ($p = 0.347$), but AVR hat larger aortic diameter ($p = 0.018$) and TAVI had larger GOA ($p = 0.027$), but

did not differ significantly from AVR regarding the GOA index ($p = 0.060$).

Blood flow patterns

All examinations resulted in diagnostic image quality. Local artifacts occurred in the proximity of the prosthetic stents similarly for TAVI and AVR. The most proximal analysis plane was therefore positioned at the sinotubular level to warrant sufficient distance from the artifact. Representative blood flow patterns of the three groups are shown in Fig. 1. Figure 2 shows a comparison between the qualitative grades for helical and vortical flow patterns. AVR revealed significantly more severe helical and vortical flow pattern than TAVI and controls, whereas TAVI had significant more vortical, but not helical flow pattern than normal subjects. There was no correlation between vortical and helical flow pattern with GOA (TAVI: $p = 0.737$ and $p = 0.951$; AVR: $p = 0.776$ and $p = 1.000$).

Blood flow eccentricity

Figure 3 summarizes the grading of the blood flow eccentricity. Controls predominantly exhibited central flow. In contrast, 11/17 TAVI patients had a markedly eccentric flow and the remaining 6 showed mildly eccentric flow. Similarly, 8/12 AVR recipients had markedly eccentric flow and the remaining 4 were mildly eccentric. AVR and TAVI differed significantly concerning the mean value of eccentricity from healthy subjects ($p < 0.001$). TAVI and AVR did not differ significantly ($p = 0.777$).

Wall shear stress

The distribution of $WSS_{systole}$ in the ascending aorta is illustrated in Fig. 4. TAVI and AVR exhibited the same distribution of $WSS_{systole}$ without relevant regional differences. Compared to controls, both TAVI and AVR revealed significantly higher $WSS_{systole}$ at the right anterior segment in the mid-ascending aorta (S2). Furthermore, WSSsystole was significantly lower in TAVI and AVR compared to controls at the left wall (S1), left-posterior wall (S2), posterior wall (S2, S3) and right-posterior wall (S3).

Discussion

In this pilot study, we used 4D-flow MRI to assess the blood flow in the ascending aorta after TAVI in comparison to AVR with stented bioprostheses as well as healthy controls. TAVI and AVR revealed significantly abnormal helical and vortical blood flow as well as $WSS_{systole}$ and a more eccentric blood flow than controls.

Both stented bioprostheses and TAVI consist of biological material mounted on a stent. Despite this similarity, AVR resulted in more distinct helical and vortical flow pattern than TAVI. This may be attributed to the lower GOA of the AVR cohort in this study, but may also reflect differences in stent design. Whereas the TAVI device is fixed passively at the calcified aorta wall, stented bioprostheses contain a sewing ring that may be an unfavorable obstacle within the blood flow, even if the implantation is done principally completely supra-annularly. The latter aspect is supported by generally lower pressure gradients of TAVI compared to AVR reported in the literature [16, 17]. Despite this potential advantage of TAVI, TAVI—as expected—also led to an abnormal blood flow pattern compared to healthy controls. At least for bicuspid aortic valves, a correlation of blood flow pattern and aortic growth rate has been shown [6]. Furthermore,

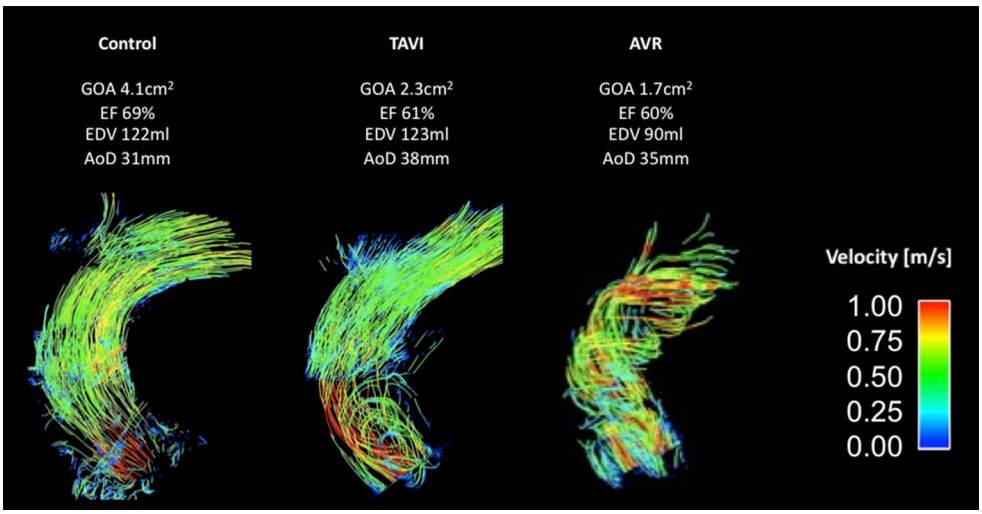

Fig. 1 Representative blood flow patterns in the ascending aorta as illustrated with pathlines. *TAVI* transcatheter aortic valve replacement, *AVR* aortic valve replacement, *GOA* effective orifice area, *EF* ejection fraction, *EDV* enddiastolic volume, *AoD* ascending aortic diameter)

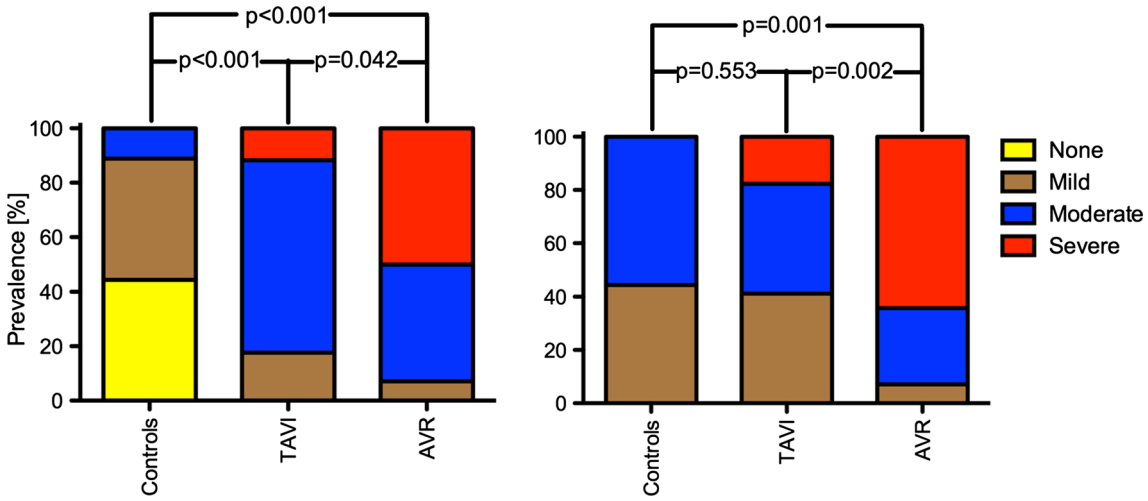

Fig. 2 Comparison of the severity of vortical (*left*) and helical (*right*) blood flow pattern

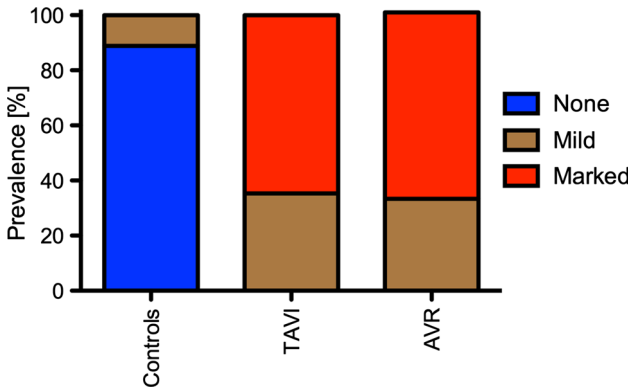

Fig. 3 Prevalence of blood flow eccentricity

novel studies that link blood flow pattern to energy loss suppose an association of blood flow pattern and cardiac afterload [7, 18]. Hence, future studies have to evaluate whether the altered blood flow of TAVI and AVR has impact on aortic and left ventricular remodeling as well.

Both TAVI and stented bioprostheses revealed an eccentric distribution of blood flow velocities in the ascending aorta compared to healthy controls, who exhibited a physiological central flow. An eccentric flow is associated with regional elevation of WSS [4, 6, 18]. This is hypothesized to contribute to an increase of the aortic diameter and aneurysm formation [6] and may be associated with a increased viscous and turbulent energy losses [7, 18].

TAVI and AVR revealed a similar eccentric distribution of WSS along the aortic circumference, which was significantly elevated and depressed in focal regions. This asymmetry clearly differed from healthy controls. Local abnormalities in WSS are thought to stimulate aneurysm formation [6, 19, 20]. In a recent study using computational fluid-dynamic analysis, WSS has been shown to be regionally elevated at the site of ascending aortic aneurysm formation [21]. Hence, it is notable that both TAVI and AVR lead to a WSS profile that imparts a regional hemodynamic abnormality at the aortic wall, which is suspected to increase the chance of an adverse vascular event. Whether the resultant WSS patterns are relevant for patients with calcified aortic stenosis, who typically have thickened and stiff aortic walls, is unclear. However, in patients with aortic regurgitation and thinned aortic wall, who may receive AVR or in the future even TAVI, this prior knowledge regarding the impact of AVR and TAVI may prove useful.

The findings of the present study highlight that 4D-flow MRI opens the door to a new dimension of information about hemodynamics. The added clinical value of this information still has to be proven in future studies. At that time, we are mainly descriptive and thereby increase the knowledge about flow patterns in the proximity of aortic prostheses. These insights may stimulate attempts to construct prosthetic devices with near-normal systolic flow behavior and to determine the best prosthetic device for the individual subject.

Limitations

(1) The control group differed from the intervention groups regarding age, orifice area and aortic dimensions. Age has a known influence on the hemodynamics in the ascending aorta as well as the aortic diameter [22, 23, 24]. Therefore, this study has to be interpreted as a pilot study. (2) Given the discrete (voxelwise) nature of the velocity data, WSS as measured by MRI is known to be underestimated.

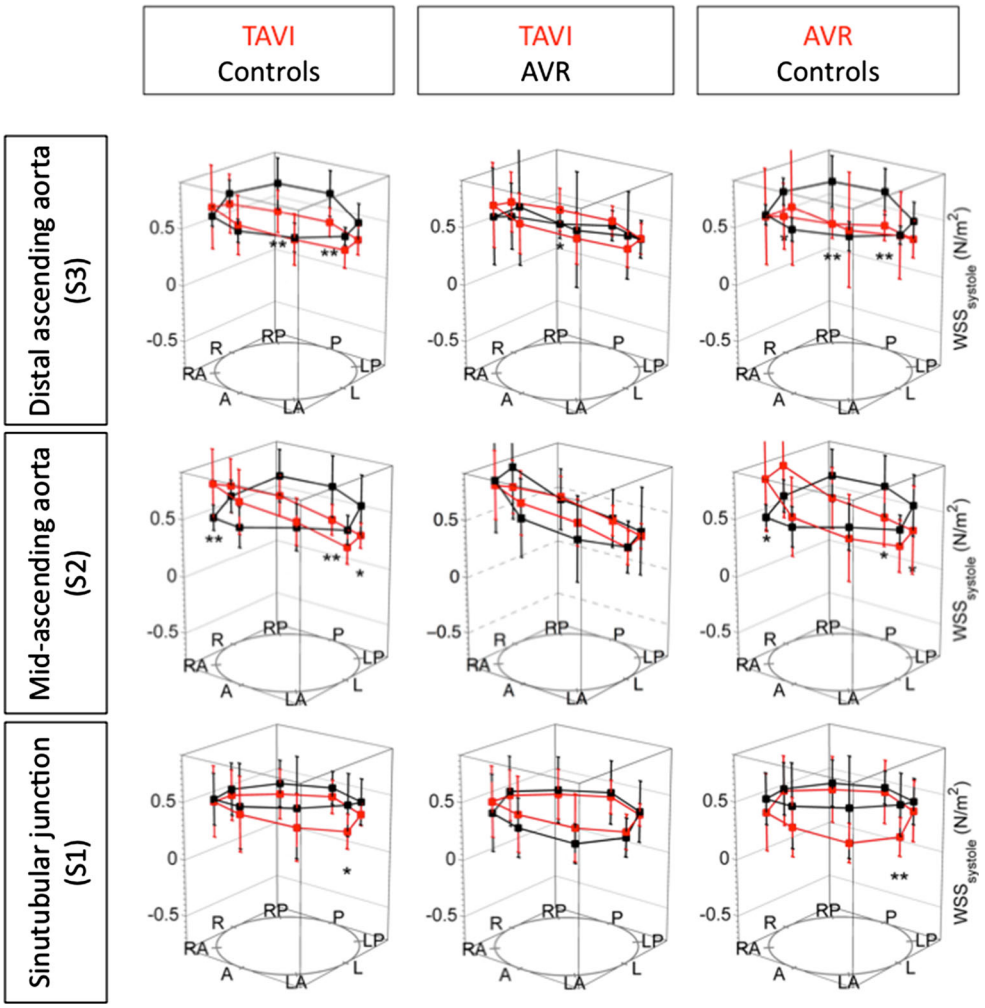

Fig. 4 Distribution of the peak wall shear stress in the ascending aorta. *R* right, *A* anterior, *L* left, *p* posterior. *asterisk* indicates $p < 0.05$ and *double asterisk* indicates $p < 0.01$

Nonetheless, the underestimation is mitigated as long as the scans are kept similar [14]. It is also imperative that careful segmentation of the vessel wall is performed, as the computation of the velocity gradients are dependent on user selection of the wall position. Previous studies have demonstrated robust intra- and inter-observer reliability and scan-rescan repeatability [25]. (3) Helical and vortical flow patterns were only assessed qualitatively. Absolute quantification of flow helicity might be superior and more objective [26]. The computation of these parameters requires specialized algorithms and/or volumetric segmentations, neither of which were available for this study. A quantitative approach should be integrated in future studies. (4) The orifice area of the TAVI prostheses was taken from literature, as direct measurement was infeasible due to artifacts. iv) This cross-sectional study was designed as a hypothesis generating pilot study, thus the enrollment was limited to small numbers. To examine the influence of the blood flow characteristics on the ascending aorta, a longitudinal study is required.

Conclusion

This pilot study demonstrated that TAVI and AVR with a stented bioprosthesis lead to altered blood flow characteristics in the ascending aorta compared to healthy controls, with more intense flow eccentricity and regional elevation of wall shear stress.

Acknowledgments We thank our technicians Kerstin Kretschel, Evelyn Polzin and Denise Kleindiest for performing the CMR scans. We also thank our study nurses Elke Nickel-Szczech and Annette Koehler as well as the other working group members for their assistance in realizing the study. This study was partly funded by the National Institutes of Health (NIH K25HL119608, R01HL115828).

Funding This study was partly funded by the National Institutes of Health (NIH K25HL119608, R01HL115828).

Compliance with ethical standards

Conflict of interest The authors declare that they have no conflict of interest.

Ethical approval All procedures were in accordance with the ethical standards of the institutional research committee and with the 1964 Helsinki declaration and its later amendments or comparable ethical standards.

References

1. Cribier A (2002) Percutaneous transcatheter implantation of an aortic valve prosthesis for calcific aortic stenosis: first human case description. Circulation 106:3006–3008
2. Leon MB, Smith CR, Mack M et al (2010) Transcatheter aortic-valve implantation for aortic stenosis in patients who cannot undergo surgery. New Engl J Med 363:1597–1607
3. Smith CR, Leon MB, Mack MJ et al (2011) Transcatheter versus surgical aortic-valve replacement in high-risk patients. New Engl J Med 364:2187–2198
4. Barker AJ, Markl M, Burk J, Lorenz R, Bock J, Bauer S, Schulz-Menger J, von Knobelsdorff-Brenkenhoff F (2012) Bicuspid aortic valve is associated with altered wall shear stress in the ascending aorta. Circ Cardiovasc Imaging 5:457–466
5. von Knobelsdorff-Brenkenhoff F, Trauzeddel RF, Barker AJ, Gruettner H, Markl M, Schulz-Menger J (2014) Blood flow characteristics in the ascending aorta after aortic valve replacement-a pilot study using 4D-flow MRI. Int J Cardiol 170:426–433
6. Hope MD, Wrenn J, Sigovan M, Foster E, Tseng EE, Saloner D (2012) Imaging biomarkers of aortic disease: increased growth rates with eccentric systolic flow. J Am Coll Cardiol 60:356–357
7. Barker AJ, van Ooij P, Bandi K, Garcia J, Albaghdadi M, McCarthy P, Bonow RO, Carr J, Collins J, Malaisrie SC, Markl M (2014) Viscous energy loss in the presence of abnormal aortic flow. Magn Reson Med 72:620–628
8. Markl M, Frydrychowicz A, Kozerke S, Hope M, Wieben O (2012) 4D flow MRI. J Magn Reson Imaging 36:1015–1036
9. Schnell S, Markl M, Entezari P, Mahadewia RJ, Semaan E, Stankovic Z, Collins J, Carr J, Jung B (2014) k-t GRAPPA accelerated four-dimensional flow MRI in the aorta: effect on scan time, image quality, and quantification of flow and wall shear stress. Magn Reson Med 72:522–533
10. Schulz-Menger JB, Bluemke DA, Bremerich J, Flamm SD, Fogel MA, Friedrich MG, Kim RJ, von Knobelsdorff-Brenkenhoff F, Kramer CM, Pennell DJ, Plein S, Nagel E (2013) Standardized image interpretation and post processing in cardiovascular magnetic resonance: Society for Cardiovascular Magnetic Resonance (SCMR) board of trustees task force on standardized post processing. J Cardiovasc Magn Reson 15:1–19
11. Spethmann S, Dreger H, Schattke S, Baldenhofer G, Saghabalyan D, Stangl V, Laule M, Baumann G, Stangl K, Knebel F (2012) Doppler haemodynamics and effective orifice areas of Edwards SAPIEN and CoreValve transcatheter aortic valves. Eur Heart J Cardiovasc Imaging 13:690–696
12. Binder RK, Webb JG, Toggweiler S, Freeman M, Barbanti M, Willson AB, Alhassan D, Hague CJ, Wood DA, Leipsic J (2013) Impact of post-implant SAPIEN XT geometry and position on conduction disturbances, hemodynamic performance, and paravalvular regurgitation. JACC Cardiovasc Interv 6:462–468
13. von Knobelsdorff-Brenkenhoff FRA, Wassmuth R, Abdel-Aty H, Schulz-Menger J (2010) Aortic dilatation in patients with prosthetic aortic valve: comparison of MRI and echocardiography. J Heart Valve Dis 19:349–356
14. Stalder AF, Russe MF, Frydrychowicz A, Bock J, Hennig J, Markl M (2008) Quantitative 2D and 3D phase contrast MRI: optimized analysis of blood flow and vessel wall parameters. Magn Reson Med 60:1218–1231
15. Hope MD, Hope TA, Crook SE, Ordovas KG, Urbania TH, Alley MT, Higgins CB (2011) 4D flow CMR in assessment of valve-related ascending aortic disease. JACC Cardiovasc Imaging 4:781–787
16. Clavel MA, Webb JG, Rodes-Cabau J, Masson JB, Dumont E, De Larochelliere R, Doyle D, Bergeron S, Baumgartner H, Burwash IG, Dumesnil JG, Mundigler G, Moss R, Kempny A, Bagur R, Bergler-Klein J, Gurvitch R, Mathieu P, Pibarot P (2010) Comparison between transcatheter and surgical prosthetic valve implantation in patients with severe aortic stenosis and reduced left ventricular ejection fraction. Circulation 122:1928–1936
17. Fairbairn TA, Steadman CD, Mather AN, Motwani M, Blackman DJ, Plein S, McCann GP, Greenwood JP (2013) Assessment of valve haemodynamics, reverse ventricular remodelling and myocardial fibrosis following transcatheter aortic valve implantation compared to surgical aortic valve replacement: a cardiovascular magnetic resonance study. Heart 99:1185–1191
18. Dyverfeldt P, Hope MD, Tseng EE, Saloner D (2013) Magnetic resonance measurement of turbulent kinetic energy for the estimation of irreversible pressure loss in aortic stenosis. JACC Cardiovasc Imaging 6:64–71
19. Mahadevia R, Barker AJ, Schnell S, Entezari P, Kansal P, Fedak PW, Malaisrie SC, McCarthy P, Collins J, Carr J, Markl M (2013) Bicuspid aortic cusp fusion morphology alters aortic 3D outflow patterns, wall shear stress and expression of aortopathy. Circulation 129:673–682
20. Cecchi E, Giglioli C, Valente S, Lazzeri C, Gensini GF, Abbate R, Mannini L (2011) Role of hemodynamic shear stress in cardiovascular disease. Atherosclerosis 214:249–256
21. Rinaudo A, Pasta S (2014) Regional variation of wall shear stress in ascending thoracic aortic aneurysms. Proc Inst Mech Eng H 228:627–638
22. Bogren HG, Mohiaddin RH, Kilner PJ, Jimenez-Borreguero LJ, Yang GZ, Firmin DN (1997) Blood flow patterns in the thoracic aorta studied with three-directional MR velocity mapping: the effects of age and coronary artery disease. J Magn Reson Imaging 7:784–793
23. Hope TA, Markl M, Wigstrom L, Alley MT, Miller DC, Herfkens RJ (2007) Comparison of flow patterns in ascending aortic aneurysms and volunteers using four-dimensional magnetic resonance velocity mapping. J Magn Reson Imaging 26:1471–1479
24. Della Corte A, Bancone C, Conti CA, Votta E, Redaelli A, Del Viscovo L, Cotrufo M (2012) Restricted cusp motion in right-left type of bicuspid aortic valves: a new risk marker for aortopathy. J Thorac Cardiovasc Surg 144:360–369
25. Markl M, Wallis W, Harloff A (2011) Reproducibility of flow and wall shear stress analysis using flow-sensitive four-dimensional MRI. J Magn Res Imaging 33:988–994
26. Lorenz R, Bock J, Barker AJ, von Knobelsdorff-Brenkenhoff F, Wallis W, Korvink JG, Bissell MM, Schulz-Menger J, Markl M (2013) 4D flow magnetic resonance imaging in bicuspid aortic valve disease demonstrates altered distribution of aortic blood flow helicity. Magn Reson Med 71:1542–1553